# Stress Corrosion Cracking of SUS304 Stainless Steel in High Temperature Water†

## – Effect of Dissolved Oxygen and Strain Rate –

Toshio ENJO* Toshio KURODA** and Yun Mo YEON***

**Abstract**

*This study was made to investigate the effects of dissolved oxygen, strain rate and solution treatment temperature on the stress corrosion cracking (SCC) of the sensitized SUS 304 stainless steel. For the specimens solution-treated at 1373K, the higher IGSCC susceptibility was attributed to Cr-depleted zone and the segregation of impurities in the high temperature water with dissolved oxygen. However, in the deaerated water, the IGSCC susceptibility decreased. As the solution treatment temperature increased, the degree of sensitization evaluated by Strauss test decreased owing to narrow Cr-depleted zone. In a slow strain rate test (SSRT), IGSCC susceptibility increased with the decrease in the strain rate in dependent of the solution treatment temperature. But, for the specimens solution-treated at 1573K, SSRT results were not correspondent with the results by Strauss test, that is, SSRT was a severe test compared with corrosion tests such as Strauss test. It was found that the electrolytic conductivity of high temperature water in SSRT was higher on sensitized specimens than that of solution-treated specimens. This increase in the electrolytic conductivity seems to be related to the pit formation at the grain boundaries of the sensitized specimens.*

KEY WORDS: (Intergranular Corrosion) (Intergranular Stress Corrosion Cracking) (Sensitization) (Solution Treatment Temperature) (Strain Rate) (Dissolved Oxygen)

## 1. Introduction

IGSCC that occurs at sensitized SUS 304 stainless steel is located in a region adjacent to the weld, and is referred to the weld heat affected zone (HAZ). IGSCC mechanism has been studied associating with the dissolved oxygen, sensitization and residual stress.[1–3] The behavior of IGSCC may be similar to that of intergranular corrosion. However, it is considered that IGSCC mechanism is different from that of intergranular corrosion. That is, intergranular corrosion occurs at all of grain boundaries, however, IGSCC occurs at localized grain boundaries. Furthermore, SCC occurs at HAZ. But, SCC hardly occurs at HAZ adjacent to the weld bond.[4] In this paper, the effects of dissolved oxygen, strain rate and solution treatment temperature on SCC susceptibilities of SUS 304 stainless steel were studied. And these results were compared with that of intergranular corrosion test.

## 2. Experimental

SCC susceptibilities of SUS 304 stainless steel were studied. **Table 1** shows the chemical composition of material used for this study. Samples were solution-treated at 1373K and 1573K for 1.8 ks in vacuum furnace. The grain sizes were 55μm (ASTM No. 5) and 220μm (ASTM No. 1) respectively. Solution-treated specimens were sensitized at 923K for 7.2 ks. SCC tests were carried out using the slow strain rate testing apparatus. The autoclave system is shown in **Fig. 1.**

**Table 1** Chemical composition.

| Material | C | Si | Mn | P | S | Ni | Cr |
|---|---|---|---|---|---|---|---|
| SUS 304 | 0.04 | 0.60 | 1.06 | 0.031 | 0.008 | 9.01 | 18.26 |

SCC specimens were finally polished with #1200 emery paper. Size and location of SCC specimen are shown in **Fig. 2.** SCC tests were carried out at various strain rate in high temperature water (562K), 8 MPa pressure of various dissolved oxygen. $N_2$ and $O_2$ gas were used to

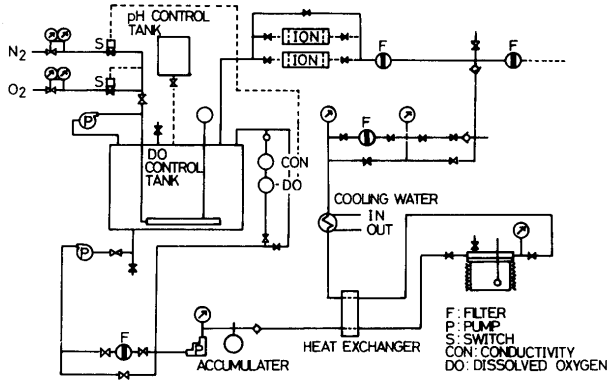


**Fig. 1** Schematic of the autoclave system.

† Received on November 4, 1986
* Professor
** Research Instructor
*** Graduate Student of Osaka University

Transactions of JWRI is published by Welding Research Institute of Osaka University, Ibaraki, Osaka 567, Japan

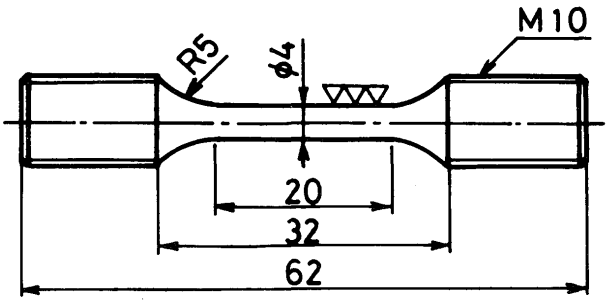


Fig. 2 Specimen for SSRT.

control dissolved oxygen. The fracture surfaces of specimens were examined using scanning electron microscope.

SCC susceptibilities were determined by means of strain ratio and R.A. of fractured samples. Transmission electron microscope was used to observe the carbides at grain boundaries. The degrees of sensitization were determined using the 10% oxalic acid test (ASTM A262A), the Strauss test (ASTM A262E), and EPR test. The oxide films on the surface of tested specimens were investigated by means of X-ray diffractometer (Target, $CuK_\alpha$).

## 3. Results and Discussions

### 3.1 The effect of solution treatment temperature on sensitization

**Figure 3** shows the grain boundary carbides of sensitized specimens. As can be seen in Fig. 3 (a) and (b), the large carbides were observed at grain boundaries as well as in matrix. These carbides at grain boundary were identified to $M_{23}C_6$ as shown in Fig. 3 (c) and (d).

Intergranular corrosion susceptibilities were determined by means of the Solomon method[5] after 10% oxalic acid test. Its susceptibilities were 95% for the sentitized specimens after heat-treated at 1373K and 80% for the sensitized specimens after heat-treated at 1573K.

**Figure 4** shows the intergranular corrosion susceptibilities of sensitized specimens after the Strauss test. As can be seen in Fig. 4 (a) and (b), the width of Cr depleted zone was narrower for the sensitized specimens after heat-treated at 1573K than that of 1373K. The depth of intergranular corrosion was deeper for the sensitized specimens after heat-treated at 1373K than that of 1573K as seen in Fig. 4 (c) and (d). Consequently, it was found that sensitization hardly accurred for the sensitized specimens after heat-treated at 1573K. Also, δ-ferrite contents were 0.2% for the sensitized specimens after heat-treated at 1373K and 0.5% for that of 1573K. It is considered that these small amounts of δ-ferrites don't affect on the intergranular corrosion susceptibilities. These results demonstrate that the sensitization hardly occurs at the HAZ adjacent to the fusion zone.

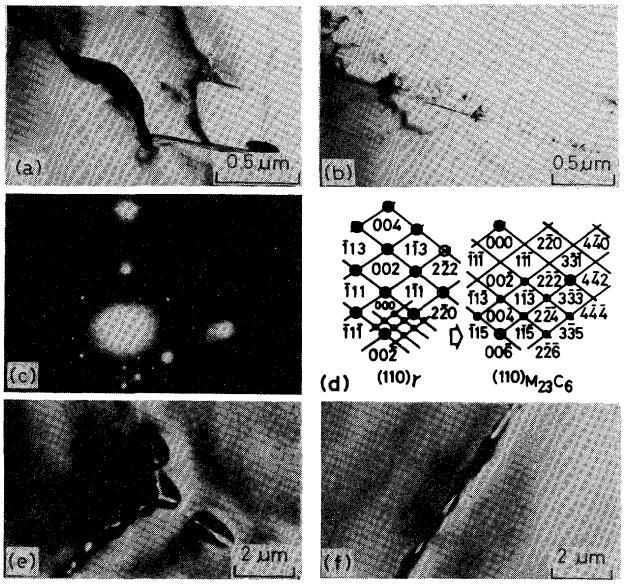


Fig. 3 Grain boundary carbides and diffraction pattern of the specimens sensitized at 923K for 7.2 ks after solutionized at 1373K (a) (c) (d) (e) and 1573K (b) (f).
(a) (b) ; Transmission electron micrograph of sensitized specimens.
(c) ; Diffraction patterns of grain boundary carbides.
(d) ; Analysis of diffraction pattern.
(e) (f) ; Grain boundary carbides by etchant of 10% hydrochloric acid alcohol.

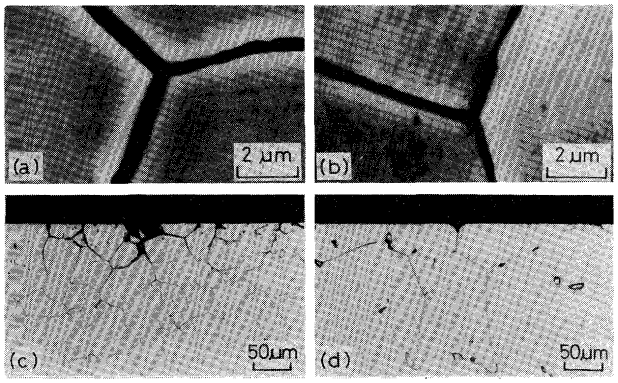


Fig. 4 Intergranular corrosion of the specimens sensitized at 923K for 7.2 ks after solutionized at 1373K (a) (c) and 1573K (b) (d).
(a) (b) ; Specimen surface after Strauss test.
(c) (d) ; Cross sectional area after Strauss test.

### 3.2 The effect of dissolved oxygen on SCC susceptibilities

**Figure 5** shows the effect of dissolved oxygen on the stress-strain curve of the sensitized specimens after heat-treated at 1373K. SCC didn't occur at 0.1 ~ 1 ppm oxygen content. However, SCC susceptibilities were greatly increased above 8 ppm oxygen content. **Figure 6** shows the effect of dissolved oxygen on the SCC susceptibilities at the strain rate of $4.17 \times 10^{-6}\ s^{-1}$. The R.A. of sensitized specimens and heat-treated specimens at 1373K was increased at the dissolved oxygen of 0.1 ~ 1 ppm. Fracture morphology showed TGSCC up to 1 ppm

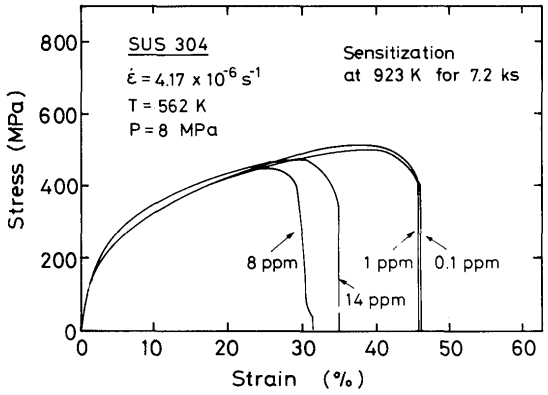


Fig. 5 The effect of dissolved oxygen on stress-strain curve.

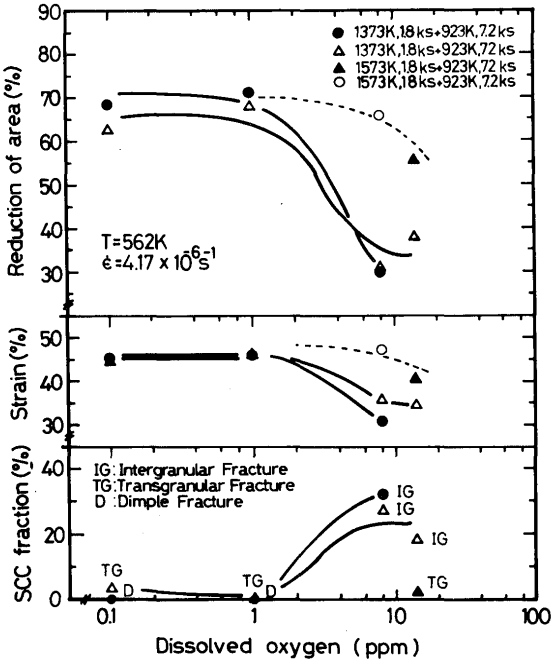


Fig. 6 The effect of dissolved oxygen on SCC susceptibility in high temperature water.

oxygen content and then it changed to IGSCC with increasing oxygen content.

It is considered that the oxide films resulting from dissolved oxygen have an important effect on SCC susceptibilities. **Figure** 7 shows the X-ray diffraction results of the sensitized sheet specimens which were exposed to various dissolved oxygen contents. As the dissolved oxygen increased, the peak height of γ-Fe (111, 200) decreased. This decrease shows that the oxide films become thick. When the dissolved oxygen was low, $Fe_2O_3$ alone was observed. At high dissolved oxygen content, $Fe_3O_4$, $Cr_2O_3$ as well as $Fe_2O_3$ were observed. These results are consistant with the studies of Hirano et al.[6] and Kuniya et al.[7] It is considered that the thick oxide films are easy to be cracked during straining, and corrosion occurs at the interface between oxide film and matrix, then, IGSCC easily occurs. As seen in Fig. 6, SCC susceptibilities of the

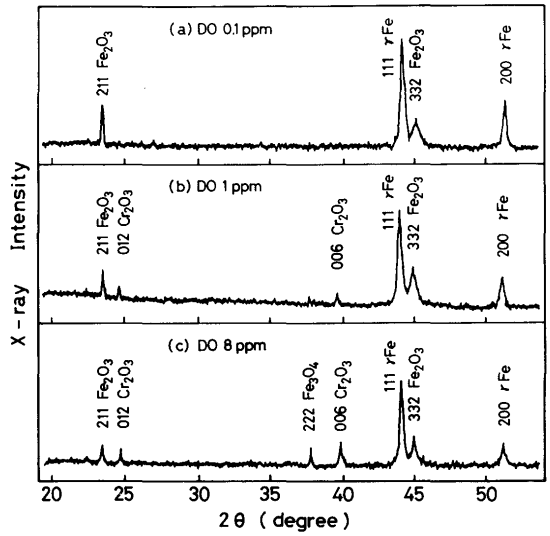


Fig. 7 X-ray diffraction patterns of the samples immersed in the high temperature water with various dissolved oxygen.

sensitized specimens after heat-treated at 1573K comparing with that of 1373K decreased above 8 ppm oxygen content. That is, as the solution treatment temperature increased, the effect of dissolved oxygen on SCC susceptibilities decreased.

### 3.3 The effect of strain rate on SCC susceptibilities

**Figure** 8 shows the effect of strain rate on SCC susceptibilities. SCC did not occur on the specimens heat-

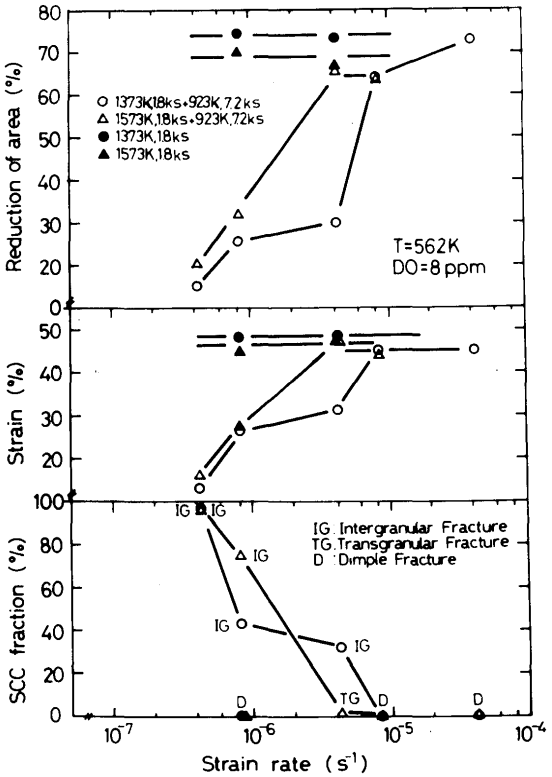


Fig. 8 The effect of strain rate on SCC susceptibility in high temperature water.

treated at 1373K and 1573K respectively. In the case of sensitized specimens, SCC susceptibilities increased with decreasing the strain rate at both solution-treated specimens.[8,9] In the sensitized specimens after heat-treated at 1373K, SCC occurred at the strain rate slower than $4.17 \times 10^{-6}\,s^{-1}$. As the solution treatment temperature was higher, SCC did not occur at same strain rate. In case of the strain rate of $8.35 \times 10^{-7}\,s^{-1}$, however, SCC occurred independent of solution treatment temperature. Also, SCC fracture ratio increased with decreasing the strain rate. **Figure 9** shows that fracture morphology varies with increasing the solution treatment temperature.

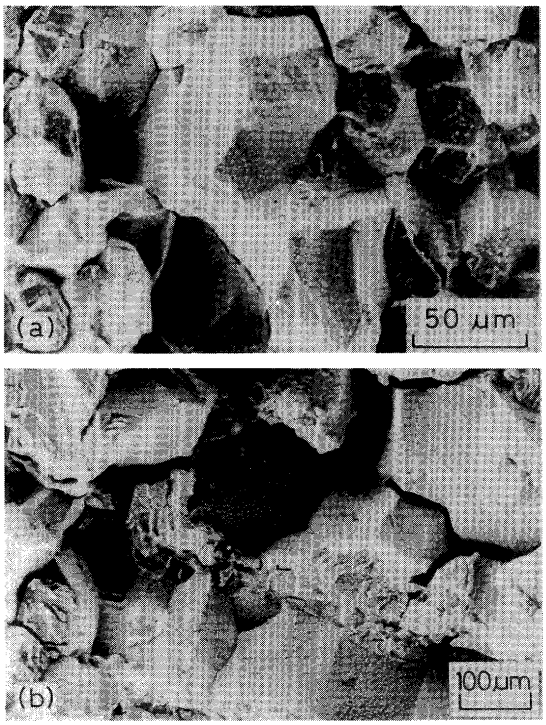


**Fig. 9** Fracture susfaces of sensitized specimens at $8.35 \times 10^{-7}\,s^{-1}$.
(a) 1373K, 1.8 ks + 923K, 7.2 ks
(b) 1573K, 1.8 ks + 923K, 7.2 ks

### 3.4 The behavior of SCC initiation

**Figure 10** shows the relationship between strain and conductivity change in pure water. Solution-treated specimens and sensitized specimens were tested. The conductivity of pure water was increased by pits or intergranular corrosion. The conductivities of the sensitized specimens after heat-treated at 1373K were constant without the effect of sensitization.

On the other hand, in the case of 1573K the conductivities of solution-treated specimens did not vary during SCC test. However, those of the sensitized specimens were increased with the strain.

In the case of $8.35 \times 10^{-7}\,s^{-1}$, the increase of conductivities of pure water began at the strain of about 10% in the solution-treated specimens. But, the conductivities

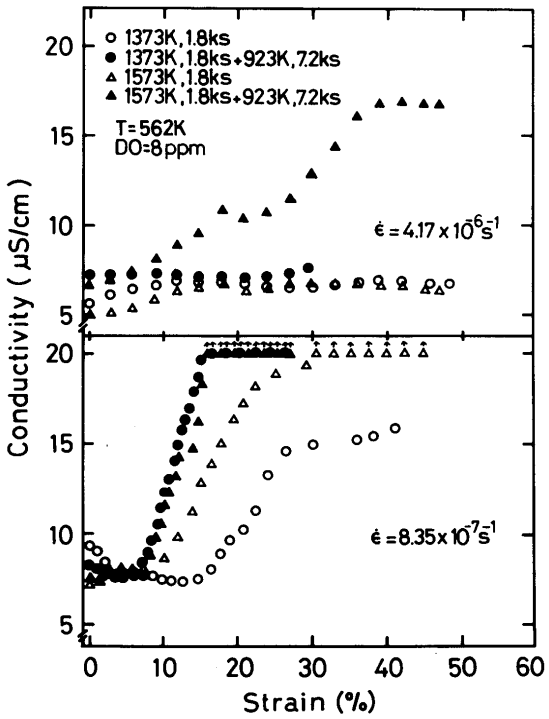


**Fig. 10** Relationship between electrolytic conductivity and strain.

of pure water for the sensitized specimens increased rapidly from the strain of about 8%. It is considered that the differences of conductivities between solution-treated specimens and sensitized specimens are due to intergranular corrosion, not pitting.

As shown in **Fig. 11**, pits were observed at both strain rates and solution treatment temperatures. However, intergranular corrosion shown in Fig. 4 (a) and (b) was not observed.

**Figure 12** shows the cross sectional microstructure. In the case of sensitized specimens after heat-treated at 1573K, pits were many observed at grain boundaries and

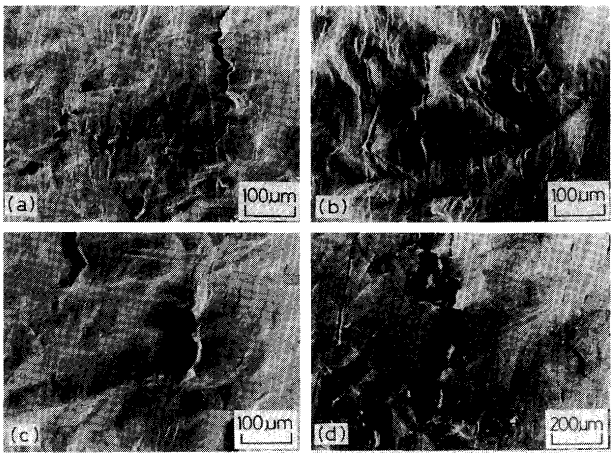


**Fig. 11** Pits and intergranular cracks on side surfaces of specimens sensitized at 923K for 7.2 ks after solutionized at 1373K (a) (c) and 1573K (b) (d) for 1.8 ks.
(a) (b) ; Test at $4.17 \times 10^{-6}\,s^{-1}$
(c) (d) ; Test at $8.35 \times 10^{-7}\,s^{-1}$

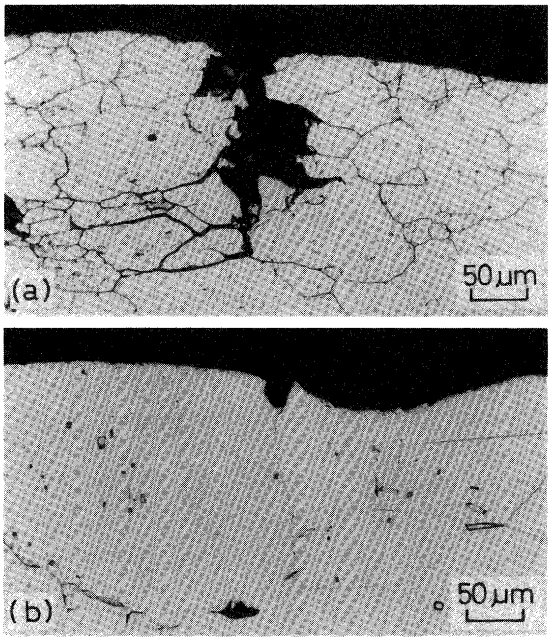


**Fig. 12** Microstructure of cross sectional area after SSRT test.
(a) Specimen sensitized at 923K for 7.2 ks after solutionized at 1373K for 1.8 ks.
(b) Specimen sensitized at 923K for 7.2 ks after solutionized at 1573K for 1.8 ks.

matrix. However, SCC was not initiated by pitting. On the other hand, in the case of the sensitized specimens after heat-treated at 1373K, there were a few pits. Furthermore, pits occurred at grain boundaries and then SCC initiated at these pits. The same results were reported in other papers.[10,11] These results were consistent with the changes of the conductivity of pure water.

The behavior of pit initiation has been discussed by means of anode polarization. In 3.5% NaCl solution (pH4), therefore, the anode polarization of sensitized specimens was investigated.

**Figure 13** shows the typical pitting on sensitized specimens. In the case of specimens after heat-treated at 1373K, pits occurred at grain boundaries. On the other hand, in the case of specimens after heat-treated at 1573K, pits occurred at matrix (A) as well as grain boundary (B). However, grain boundaries were not preferentially corroded. The behavior of pit initiation in this solution were similiar to that of pure water as shown in **Fig. 12**. It is considered that the pits observed in this solution also occurs in SCC test. That is, the conductivity of pure water was increased in the sensitized specimens after heat-treated at 1573K, but, SCC did not occur as shown in Fig. 8. These means that the pits are not the path of SCC. Also, in the case of specimens heat-treated at 1373K, the conductivity of pure water did not vary. However, SCC remarkably occurred. Provided the pits are presented at grain boundary, SCC greatly occur. Therefore, it is considered that the SCC is associated with the initiation and

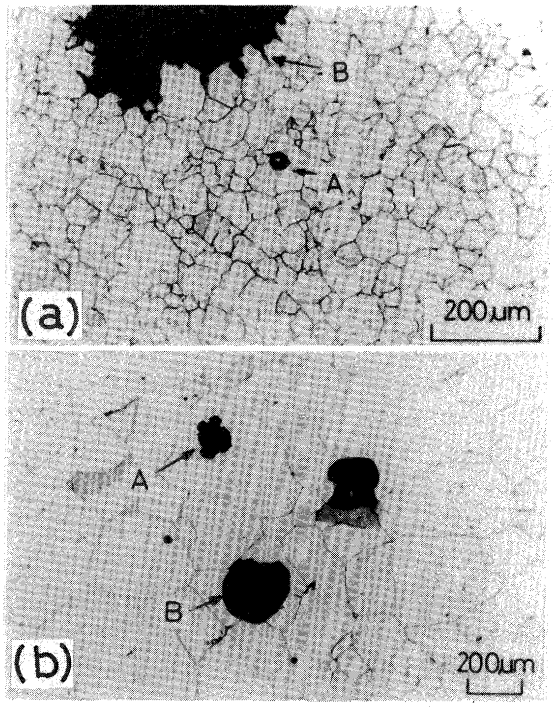


**Fig. 13** Typical pitting on sensitized specimens.
(a) 1373K, 1.8 ks + 923K, 7.2 ks
(b) 1573K, 1.8 ks + 923K, 7.2 ks

growth of pits, not with the number of pits.

### 3.5 The relationship between intergranular corrosion and SCC

**Figure 14** shows the cross section of sensitized specimens after SCC test and Strauss test. In the case of the sensitized specimens after heat-treated at 1373K, intergranular corrosion occurred near the surface of specimens. But, SCC was observed along the grain boundaries as shown in Fig. 14 (a). This means that SCC is accelerated by means of stress rather than intergranular corrosion. In

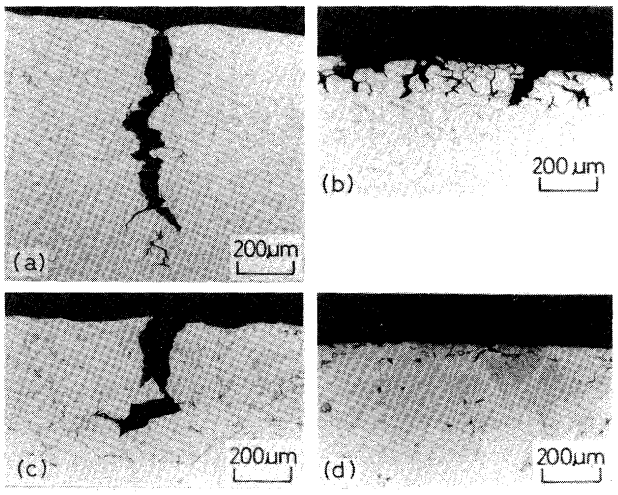


**Fig. 14** Comparison of sensitized specimens in SSRT (a) (c) and A262E (b) (d).
(a) (b) ; 1373K, 1.8 ks + 923K, 7.2 ks
(c) (d) ; 1573K, 1.8 ks + 923K, 7.2 ks

the case of the sensitized specimens after heat-treated at 1573K, SCC occurred at the narrow Cr-depleted zone. However, on the specimens of 1573K, intergranular corrosion didn't occur at the Strauss test although the 80% of grain boundaries was attacked in A262A test. It is considered that the segregation behavior of impurities in the specimens heat-treated at 1373K is different from that of 1573K.[12] To observe the effect of impurities at grain boundaries, the specimens were annealed at 1373K for 1.8 ks after heat-treated at 1573K for 1.8 ks.

**Figure 15** shows the results of intergranular corrosion and pitting. The width of Cr-depleted zone was broader than that shown in Fig. 4 (b). Also, the pits which occurred at grain boundary were proceded along the grain boundaries as shown in Fig. 13 (a). This phenomenon indicates that the impurities segregate at grain boundary during annealing at 1373K.

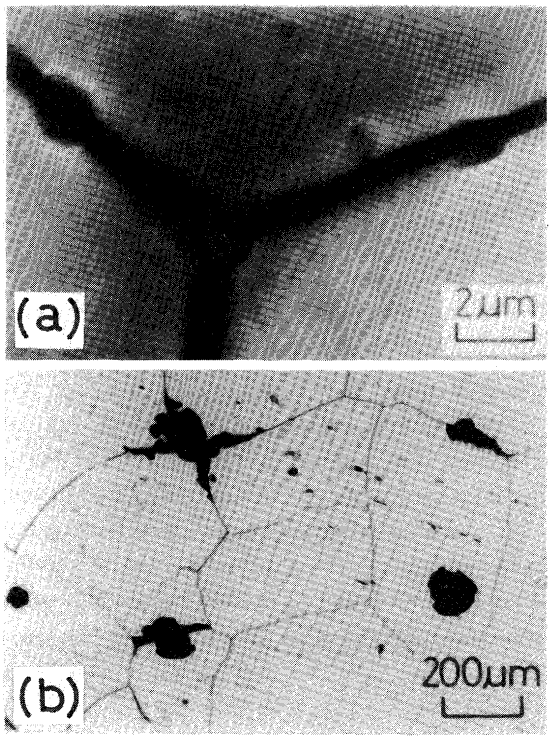


Fig. 15 Morphology of intergranular corrosion by Strauss test (a) and pitting by anodic polarization (b).

P and S are considered as the impurities. Briant[13] has proposed that intergranular corrosion did not occur at 0.03Wt%S, but at 0.06Wt%P. Furthermore, Danyluk et al.[14] have found that intergranular corrosion occurred if S and P are 0.087Wt% and 0.03Wt% respectively. In this study, P and S were included 0.031Wt% and 0.008Wt% respectively. Therefore, it is considered that S does not affect on intergranular corrosion susceptibility, but the segregation of 0.031Wt%P to grain boundaries may be affect on the intergranular corrosion susceptibility.

Based on these results, it was found that pits occurred at grain boundary in the case of sensitized specimens after heat-treated at 1373K, and then SCC was resulted from these pits at the small amount of strain. Also, it is considered that pits occurred at grain boundaries and matrix for the sensitized specimens after heat-treated at 1573K, but, IGSCC did not occur in terms of these pits.

## 4. Conclusions

In this paper, the SCC susceptibilities of SUS 304 stainless steel were studied using the slow strain rate test (SSRT) in high temperature pure water. It was investigated of the effects of the dissolved oxygen, the strain rate and the solution treatment temperature on the SCC susceptibilities. The obtained results are as follows.

(1) The large carbides precipitated at grain boundary were observed in the sensitized specimens after-treated at 1373K. On the other hand, the carbides were small and were also observed in matrix and grain boundary in the case of sensitized specimens after heat-treated at 1573K. Sensitization phenomenon was hardly observed on the solution-treated specimens at 1573K than that of treated at 1373K.

(2) In the sensitized specimens after heat-treated at 1373K, SCC occurred in high temperature pure water containing 8 ppm oxygen content, but not at 0.1 ~ 1 ppm oxygen content. In the case of sensitized specimens after heat-treated at 1573K, however, SCC hardly occurred under the same experimental condition.

(3) SCC was not observed at solution-treated specimens. In sensitized specimens, SCC did not occur with increasing the solution treatment temperature. However, SCC occurred independent of the solution treatment temperature as the strain rate decreased to $8.35 \times 10^{-7} s^{-1}$. The SCC fracture ratio was increased with decreasing the strain rate. Moreover, the fracture mode varied to IGSCC from TGSCC.

(4) Comparing the SCC susceptibilities with the conductivities of pure water, the conductivities increased for the sensitized specimens after heat-treated at 1573K and a number of pits were observed. But, SCC has not been proceded from these pits. In the case of the specimens heat-treated at 1373K, the conductivities of pure water have not varied in both the solution-treated specimens and the sensitized specimens during SCC test. However, SCC greatly occurred if pits was produced at the grain boundaries for the sensitized specimens.

### References

1) Y. Mukai, M. Murata, N. Tamaoki, and H. Kazaoka: Quart. J. of Japan Weld. Soc, 3-2 (1985), 422 (in Japanese).

2) Y. Mukai, and M. Murata: J. of Soc, of Mat. Sci, Japan. 34-381 (1985), 697 (in Japanese).

3) H. D. Solomon, M. J. Povich and T. M. Devine: ASTM STP 665, (1979), 132.

4) B. Vyas and H. S. Isaacs: ASTM STP 656, (1978), 133.

5) H. D. Solomon: Corrosion, 40-9 (1984), 493.

6) H. Hirano, M. Mayuzumi and T. Kurosawa: Boshoku Gijutsu, 31-8, (1982), 517 (in Japanese).

7) J. Kuniya, M. Kanno, I. Masaoka and R. Sasaki: Boshoku Gijutsu, 32-11, (1983), 649 (in Japanese).

8) H. Tsuge, J. Murayama and H. Nagano: Tetsu to Hagane, 69-16, (1983), 2068 (in Japanese).

9) M. Hishida and H. Nakada: Corrosion, 33-9, (1977), 332.

10) P. L. Andresen: Corrosion, 38-1, (1982), 53.

11) G. Cragnolimo, L. F. Lin and Z. S. Smialowska: Corrosion, 37-6, (1981), 312.

12) J. S. Armijo: Corrosion Science, 7, (1967), 143.

13) C. L. Briant: Corrosion, 36-9, (1980), 497.

14) S. Danyluk, J. H. Hong and I. Wolke: Corrosion, 40-11, (1984), 598.